
Q-Insight: Understanding Image Quality via Visual Reinforcement Learning

Weiqli Li¹, Xuanyu Zhang¹, Shijie Zhao²[✉], Yabin Zhang², Junlin Li², Li Zhang², Jian Zhang¹[✉]

¹ School of Electronic and Computer Engineering, Peking University

² ByteDance Inc.

Abstract

Image quality assessment (IQA) focuses on the perceptual visual quality of images, playing a crucial role in downstream tasks such as image reconstruction, compression, and generation. The rapid advancement of multi-modal large language models (MLLMs) has significantly broadened the scope of IQA, moving toward comprehensive image quality understanding that incorporates content analysis, degradation perception, and comparison reasoning beyond mere numerical scoring. Previous MLLM-based methods typically either generate numerical scores lacking interpretability or heavily rely on supervised fine-tuning (SFT) using large-scale annotated datasets to provide descriptive assessments, limiting their flexibility and applicability. In this paper, we propose **Q-Insight**, a reinforcement learning-based model built upon group relative policy optimization (GRPO), which demonstrates strong visual reasoning capability for image quality understanding while requiring only a limited amount of rating scores and degradation labels. By jointly optimizing score regression and degradation perception tasks with carefully designed reward functions, our approach effectively exploits their mutual benefits for enhanced performance. Extensive experiments demonstrate that Q-Insight substantially outperforms existing state-of-the-art methods in both score regression and degradation perception tasks, while exhibiting impressive zero-shot generalization to comparison reasoning tasks. Code will be available at <https://github.com/lwq20020127/Q-Insight>.

1 Introduction

Image quality assessment (IQA) is a fundamental task in computer vision, critical for optimizing algorithms, enhancing user experiences, and verifying content authenticity across diverse domains, such as image processing [38, 21, 10, 51] and AI-generated content (AIGC) [35, 7]. Traditional IQA methods rely heavily on hand-crafted metrics, either through reference-based comparisons [47] or statistical measures of natural image properties [62]. However, these approaches typically focus on local image characteristics and fail to comprehensively capture global visual quality, limiting their reliability in complex real-world scenarios. More recently, deep learning-based IQA models [44, 18] have emerged, utilizing neural networks to learn hierarchical image representations. Nevertheless, these methods struggle to face significant challenges in out-of-distribution (OOD) generalization.

With recent advances in multi-modal large language models (MLLMs) [22, 1, 45], researchers have begun to leverage these models' extensive world knowledge and perceptual abilities to enhance IQA performance and broaden its applicability [51, 58, 57, 56, 49]. Existing MLLM-based IQA methods generally fall into two categories: score-based methods, such as Q-Align [51] and DeQA-Score [56], and description-based methods, exemplified by DepictQA [58] and DepictQA-Wild [57].

[✉]Project Lead. ✉: Corresponding authors, zhaoshijie.0526@bytedance.com, zhangjian.sz@pku.edu.cn.

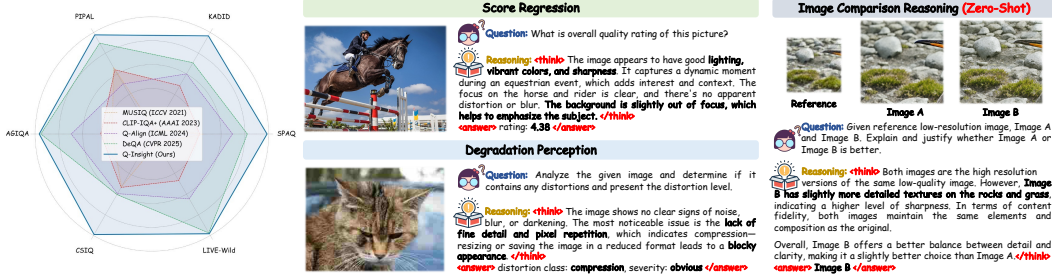


Figure 1: We present the PLCC comparison between proposed Q-Inight and other IQA metrics on the left and list the applications of our Q-Inight on the right. Q-Inight shows significant performance on the out-of-domain datasets (e.g. CSIQ) compared to methods like DeQA, while simultaneously achieving score regression, degradation perception, and zero-shot image comparison reasoning tasks.

Score-based methods transform discrete tokens into continuous quality scores, thereby improving adaptability but typically sacrificing interpretability and neglecting MLLMs’ intrinsic reasoning and descriptive capabilities. Meanwhile, **simply regressing a quality score may not be meaningful in certain scenarios**, as image quality scores are subjective, inherently biased, and lack uniform standards across different datasets and content types. For example, when evaluating AIGC-generated data, unusual visual effects and vibrant colors often imply better quality. However, for evaluating super-resolution results, these same features are often considered too painterly, losing the image’s authenticity and fidelity. Conversely, description-based methods produce detailed textual explanations of image degradations and comparative assessments, ensuring interpretability yet heavily depending on extensive textual depiction for supervised fine-tuning. Moreover, these models cannot output precise scores, making them unsuitable when used as loss functions or for performing accurate ranking of image quality. Consequently, integrating **numerical scoring** and **descriptive reasoning** into a unified, interpretable MLLM-based IQA framework remains an essential yet unresolved challenge.

In this paper, we move towards a comprehensive understanding of image quality by addressing tasks such as image description, aesthetic and compositional evaluation, degradation perception, and comparative reasoning across images. Rather than teaching the large model “*How to score images*”, we aim to inspire it “*How to reason deeply and formulate insightful perspectives on image quality metrics during scoring*”. To this end, we resort to Group Relative Policy Optimization (GRPO) [37], a reinforcement learning framework inspired by DeepSeek-R1 [14]. GRPO has recently shown to be highly effective in large language models (LLMs). It uses heuristic reward signals to efficiently guide LLMs in uncovering their intrinsic reasoning capabilities, removing extensive reliance on annotated reasoning chains or additional value models. Recently, researchers have also successfully adapted GRPO to vision-language tasks, including few-shot object detection, reasoning grounding [24], and medical analysis [33]. In the context of image quality understanding, the introduction of GRPO provides at least three distinct advantages: (1) no reliance on massive textual training data, (2) strong generalization to OOD evaluated images, and (3) high diversity in supporting multiple tasks. These benefits align well with our goal of developing a generalized image quality understanding agent.

Specifically, we design **Q-Inight** upon the GRPO framework. In our Q-Inight, we jointly optimize score regression and degradation perception tasks, and carefully design three reward functions: a verifiable score reward for the score regression task, and degradation classification and intensity perception rewards for the degradation perception task. Consequently, Q-Inight effectively exhibits robust reasoning performance in image quality assessment tasks using only limited Mean Opinion Scores (MOS) and degradation labels. As shown in Fig. 1, our Q-Inight shows exceptional improvements on OOD datasets, while demonstrating comprehensive quality perception and sophisticated reasoning abilities, such as recognizing that a slightly out-of-focus background, which might conventionally be perceived as undesirable, actually helps emphasize the main subject of the image. Our empirical investigation reveals that: (1) training solely with score labels results in poor perception of image detail degradations (e.g., JPEG compression), while jointly training with the degradation perception task significantly enhances the model’s sensitivity to such degradations, and (2) score regression and degradation perception tasks are mutually beneficial. Extensive experiments across score regression and degradation perception tasks demonstrate that Q-Inight consistently outperforms existing model-based IQA metrics as well as SFT-driven large language models. Moreover, it

exhibits impressive zero-shot generalization on unseen tasks, such as image comparison reasoning, highlighting the robustness and versatility of our method. In summary, our contributions are:

- (1) We propose Q-Insight, the first reasoning-style model specifically designed for comprehensive image quality understanding. Unlike previous methods that depend heavily on detailed textual descriptions for supervised fine-tuning (SFT), our approach achieves superior understanding capability using only limited mean opinion scores or degradation labels.
- (2) We introduce a unified framework that jointly optimizes image quality rating and degradation perception, revealing mutual benefits across tasks. Within this framework, we develop three specialized rewards, including verifiable score reward, degradation classification and intensity perception rewards, enabling the GRPO framework to effectively generalize to low-level vision applications.
- (3) Extensive experiments across diverse datasets and IQA tasks demonstrate that Q-Insight consistently outperforms existing model-based IQA metrics as well as SFT-driven large language models. Moreover, it exhibits impressive zero-shot generalization on unseen tasks, such as reference-based image comparison reasoning, highlighting the robustness and versatility of our method.

2 Related Work

Score-based IQA methods include full-reference and no-reference approaches. Full-reference methods [47, 39, 63] assess image quality by comparing distorted images with high-quality references using traditional metrics (e.g., SSIM [47]) or advanced deep-learning-based metrics [3, 4, 9, 8, 12, 34] like LPIPS [64]. Non-reference methods evaluate quality without reference images, shifting from traditional handcrafted statistics [26, 27, 28, 29, 30, 36] to deep-learning-derived quality priors [17, 18, 23, 32, 41, 71, 72, 42, 46]. Recent multi-modal large language model (MLLM)-based methods, such as Q-Align [51] and DeQA-Score [56], leverage MLLMs’ knowledge and perceptual abilities to produce accurate scores. However, they sacrifice the intrinsic descriptive capabilities of MLLMs.

Description-based IQA methods utilize the foundational knowledge of MLLMs to deliver detailed qualitative assessments and improved interpretability [48, 50, 58, 57, 52, 5, 68, 69, 67]. For instance, Q-Bench [48] and Q-Instruct [50] enhance the low-level perceptual capabilities of MLLMs through specialized datasets and tailored evaluation strategies. Co-Instruct [52] specifically focuses on comparative quality assessments among multiple images. Approaches such as DepictQA [58] and DepictQA-Wild [57] handle both single-image and paired-image evaluations across full-reference and no-reference scenarios. Q-Ground [5] emphasizes a detailed visual quality analysis through visual grounding. However, these methods are highly dependent on extensive textual annotations for supervised fine-tuning, leading to considerable costs in human labor or GPT token consumption.

Reinforcement learning (RL) has emerged as an effective strategy to enhance the reasoning performance of LLMs through feedback-driven refinement [6, 40, 37, 53, 55, 16, 66]. Methods like RLHF [31] and RLAIIF [2] employ human or AI-generated feedback to refine model behavior. In vision-language tasks, RL has successfully been employed to align model predictions closely with human preferences and reduce hallucinations [43, 59, 60, 70]. Recently, DeepSeek-R1-Zero [14] introduced Group Relative Policy Optimization (GRPO)[37], leveraging rule-based rewards to strengthen reasoning capabilities without supervised fine-tuning. Furthermore, Visual-RFT[24] applied GRPO to visual grounding, and Med-R1 [33] adopted GRPO for medical reasoning tasks. R1-VL [61] extends GRPO through step-wise optimization for multi-modal reasoning. Distinctly, our Q-Insight is the first to integrate RL-based strategies into the foundational visual quality understanding model. It jointly trains on multiple tasks and demonstrates mutually beneficial effects among them.

3 Methodology

3.1 Preliminaries

Group Relative Policy Optimization (GRPO) is an innovative reinforcement learning paradigm that has been widely used in models such as DeepSeek R1-Zero, achieving excellent results. Unlike PPO, which requires an explicit critic model to evaluate the performance of the policy model, GRPO directly computes the advantage by comparing a group of responses sampled from the policy model, greatly reducing the computational burden. Specifically, given a query q , GRPO samples N distinct responses

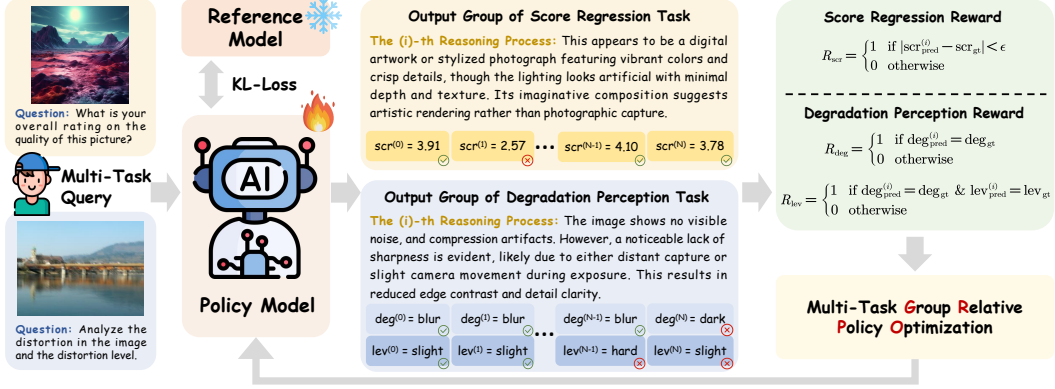


Figure 2: **Overview of the proposed Q-Insight framework.** The policy model receives queries from multiple tasks and generates corresponding groups of responses accompanied by explicit reasoning steps. Task-specific reward functions (R_{scr} , R_{deg} , and R_{lev}) are then computed, and the policy model is subsequently optimized jointly using the multi-task group relative policy optimization algorithm.

$\{o^{(1)}, o^{(2)}, \dots, o^{(N)}\}$ from the old policy $\pi_{\theta_{old}}$. Then, the method performs the corresponding actions and receives the respective rewards $\{r^{(1)}, r^{(2)}, \dots, r^{(N)}\}$ according to the task-specific rules. By calculating the mean and standard deviation of the rewards, the relative advantages of each response can be obtained as follows:

$$\hat{A}^{(i)} = \frac{r^{(i)} - \text{mean}(\{r^{(1)}, r^{(2)}, \dots, r^{(N)}\})}{\text{std}(\{r^{(1)}, r^{(2)}, \dots, r^{(N)}\})}, \quad (1)$$

where $\hat{A}^{(i)}$ represents the normalized relative quality of the i -th answer. Overall, GRPO guides the policy model to prioritize higher-quality answers that receive higher reward values within the group.

After obtaining the advantage $\hat{A}^{(i)}$, GRPO calculates the ratio of the probabilities of each response under the new policy $\pi_{\theta_{new}}$ and the old policy $\pi_{\theta_{old}}$, denoted as $\text{ratio}^{(i)}$. To prevent overly large updates to the model and stabilize training, GRPO restricts the $\text{ratio}^{(i)}$ to the range $[1 - \delta, 1 + \delta]$. To further maintain closeness to the reference distribution π_{ref} , a KL divergence penalty weighted by β is adopted. Finally, the optimization objective of GRPO can be formulated as follows:

$$\mathcal{J}(\theta) = \mathbb{E}_{[q \sim Q, o^{(i)} \sim \pi_{\theta_{old}}]} \left\{ \min \left[\text{ratio}^{(i)}, \text{clip} \left(\text{ratio}^{(i)}, 1 - \delta, 1 + \delta \right) \right] \hat{A}^{(i)} - \beta \cdot \mathbb{D}_{KL}[\pi_{\theta_{new}} || \pi_{ref}] \right\},$$

with $\text{ratio}^{(i)} = \pi_{\theta_{new}}(o^{(i)} | q) / \pi_{\theta_{old}}(o^{(i)} | q),$ (2)

where Q denotes the candidate question set, \mathbb{D}_{KL} denotes the KL regularization. π_{ref} is typically a frozen pre-trained M-LLM. In a nutshell, GRPO effectively integrates consistent policy updates and strong reward signals in a balanced and controlled way.

3.2 Overview of Q-Insight

The overall framework of Q-Insight is illustrated in Fig. 2. During training, we jointly optimize two tasks: score regression and degradation perception. Specifically, the multi-modal input for each task comprises an image paired with a task-specific question. Given these inputs, the policy model π_{θ} generates groups of answers, each accompanied by explicit reasoning steps. Subsequently, each answer is evaluated using its corresponding reward function: R_{scr} for score regression, and R_{deg} and R_{lev} for degradation perception. After computing rewards for each group of answers, the policy model is optimized jointly via the multi-task GRPO algorithm. Additionally, a KL-divergence loss is applied to constrain deviations between the policy model π_{θ} and the reference model π_{ref} . During inference, the trained Q-Insight generates coherent reasoning processes and outputs precise answers. Further details regarding multi-task GRPO and data construction are provided in Sec. 3.3 and Sec. 3.4.

Table 1: **Prompts for Different Tasks.** The system prompt is shared across all tasks, while task-specific prompts are additionally designed for each individual task.

System Prompt: A conversation between User and Assistant. The user asks a question, and the Assistant solves it. The assistant first thinks about the reasoning process in the mind and then provides the user with the answer. The reasoning process and answer are enclosed within `<think>` `</think>` and `<answer>` `</answer>` tags, respectively, i.e., `<think>` reasoning process here `</think>``<answer>` answer here `</answer>`.

Prompt for Score Regression Task: What is your overall rating on the quality of this picture? The rating should be a float between 1 and 5, rounded to two decimal places, with 1 representing very poor quality and 5 representing excellent quality. Return the final answer in JSON format with the following keys: "rating": The score.

Prompt for Degradation Perception Task: Analyze the given image and determine if it contains any of the following distortions: "noise", "compression", "blur", or "darken". If a distortion is present, classify its severity as "slight", "moderate", "obvious", "serious", or "catastrophic". Return the result in JSON format with the following keys: "distortion_class": The detected distortion (or "null" if none). and "severity": The severity level (or "null" if none).

Prompt for Reference-Based Zero-shot Comparison Reasoning: Given reference low-quality image: `<ref_image>`, Image A: `<image_A>` and Image B: `<image_B>`. Image A and Image B are results from two resolution methods. Explain and justify whether Image A or Image B is better. You should think from the following aspects: (1) Content fidelity and consistency with the reference image and (2) overall quality. Your answer should be "Image A" or "Image B".

3.3 Multi-Task Group Relative Policy Optimization

Reward design is crucial for RL-based approaches, as it allows Q-Inspire to iteratively enhance its reasoning capabilities. Specifically, given each input data pair, the policy model π_θ generates a group of N responses, denoted as $\{o^{(i)}\}_{i=1}^N$. We then evaluate these response groups using our designed reward functions to obtain $\{r^{(i)}\}_{i=1}^N$. This includes a general format reward shared by all tasks, along with task-specific rewards customized to the distinct characteristics of each task.

Format reward evaluates whether the reasoning steps are properly enclosed within “`<think>`” and “`</think>`” tags, and the final answer is correctly enclosed within “`<answer>`” and “`</answer>`” tags. Additionally, the content inside “`<answer>`” must follow a JSON-like format, beginning with “{”, ending with “}”, and containing no additional “{” or “}” characters internally. Finally, a reward score $r_{\text{fmt}}^{(i)}$ for i -th response of 1 is assigned if all these conditions are satisfied. Otherwise, the reward is 0.

Rewards for score regression task. A standard way to quantify image quality is using the Mean Opinion Score (MOS). Inspired by DeepSeek-R1 [14], which leverages the final answers of math problems as a guide to promote deeper reasoning, we similarly employ MOS scores as general targets to encourage detailed reasoning and critical thinking when assessing image quality. Denoting the predicted score of the i -th response as $\text{scr}_{\text{pred}}^{(i)}$ and the ground-truth score as scr_{gt} , we design a verifiable score reward function R_{scr} as follows. The reward value $r_{\text{scr}}^{(i)}$ for the i -th response is determined by:

$$r_{\text{scr}}^{(i)} = 1 \quad \text{if } |\text{scr}_{\text{pred}}^{(i)} - \text{scr}_{\text{gt}}| < \epsilon, \text{ otherwise } 0, \quad (3)$$

where ϵ is a predefined threshold, allowing the model’s score predictions to fluctuate within an acceptable range rather than requiring exact accuracy. Thus, the predicted score receives a reward of 1 if it falls within the threshold ϵ of the ground-truth MOS, and 0 otherwise.

Rewards for degradation perception task. In the degradation perception task, the model is expected to predict both the distortion class and its corresponding level. Denoting the predicted distortion class and level of the i -th response as $\text{deg}_{\text{pred}}^{(i)}$ and $\text{lev}_{\text{pred}}^{(i)}$ respectively, we define the degradation classification reward as follows. The reward value $r_{\text{deg}}^{(i)}$ is determined by:

$$r_{\text{deg}}^{(i)} = 1 \quad \text{if } \text{deg}_{\text{pred}}^{(i)} = \text{deg}_{\text{gt}}, \text{ otherwise } 0. \quad (4)$$

This means the predicted distortion class receives a reward of 1 if correct, and 0 otherwise. Similarly, the distortion-level reward $r_{\text{lev}}^{(i)}$ is determined by:

$$r_{\text{lev}}^{(i)} = 1 \quad \text{if } \text{deg}_{\text{pred}}^{(i)} = \text{deg}_{\text{gt}} \text{ and } \text{lev}_{\text{pred}}^{(i)} = \text{lev}_{\text{gt}}, \text{ otherwise } 0. \quad (5)$$

Thus, the predicted distortion level earns a reward of 1 only if both the predicted class and the level exactly match the ground truth; otherwise, it receives 0.

Finally, the overall reward of i -th response is calculated as:

$$r^{(i)} = r_{\text{fmt}}^{(i)} + \mathbb{1}_{\text{scr}} \cdot r_{\text{scr}}^{(i)} + \mathbb{1}_{\text{deg}} \cdot \left(\alpha_1 \cdot r_{\text{deg}}^{(i)} + \alpha_2 \cdot r_{\text{lev}}^{(i)} \right), \quad (6)$$

where $\mathbb{1}_{\text{scr}}$ equals 1 if the score regression task is selected (and 0 otherwise), and similarly, $\mathbb{1}_{\text{deg}}$ equals 1 if the degradation perception task is selected (and 0 otherwise). After computing rewards for all generated responses $\{r^{(1)}, r^{(2)}, \dots, r^{(N)}\}$, the policy model is updated following Eqs. (1) and (2).

3.4 Data Construction

We construct multi-modal training data to jointly train Q-Insight on the score regression and degradation perception tasks. The prompts designed for each task are detailed in Tab. 1. Specifically, a general system prompt is shared across tasks, which encourages the model to explicitly output its reasoning process and provide structured responses. This general prompt is supplemented by task-specific prompts tailored for score regression and degradation perception, respectively. For the score regression task, the input includes a task-specific prompt and the image to be rated, with the Mean Opinion Score (MOS) serving as the ground-truth. In the degradation perception task, the input consists of a prompt and an image characterized by a specific distortion class and severity level. We define five distortion categories: “noise”, “blur”, “JPEG”, “darken”, and “null”, where “null” indicates no distortion. Each distortion type has five severity levels: “slight”, “moderate”, “obvious”, “serious”, and “catastrophic”. The distortion class and corresponding severity level constitute the ground-truth labels. Additionally, for the zero-shot comparative reasoning scenario, inputs include a prompt, two images to be compared, and an optional reference image.

4 Experiments

4.1 Experimental Setup

Datasets and Metrics. For the score regression task, we use diverse IQA datasets across four categories: (a) in-the-wild datasets, including KonIQ [15], SPAQ [10], and LIVE-Wild [11]; (b) synthetic distortion datasets, including KADID [21] and CSIQ [19]; (c) model-processed distortions, including PIPAL [13]; and (d) AI-generated images from AGIQA [20]. Following [56], we split KonIQ into training and test sets, with approximately 7000 training images. Mean Opinion Scores (MOS) across these datasets are normalized into the range $[1, 5]$. The remaining datasets are exclusively used to evaluate the model’s out-of-distribution (OOD) generalization capability. For the degradation perception task, we randomly select 7000 images from DQ-495K [57] that contain a single distortion for training, with an additional 1000 images reserved for testing. We adopt the pearson linear correlation coefficient (PLCC) and spearman rank-order correlation coefficient (SRCC) as metrics to evaluate performance on the score regression task, following [18, 51, 56]. For the degradation perception task, we employ distortion class accuracy and degradation level accuracy as evaluation metrics.

Implementation Details. We adopt Qwen-2.5-VL-7B [1] as our base model. In the GRPO algorithm, the generation number N is set to 8, while the weights α_1 and α_2 are set to 0.25 and 0.75, respectively. The threshold ϵ is set to 0.35. We employ AdamW [25] as the optimizer, using an initial learning rate of 1×10^{-6} that linearly decays during training. The model is trained for 10 epochs with a total batch size of 128. Training is completed in approximately one day using 16 NVIDIA A100 GPUs.

4.2 Score Regression

We first evaluate our Q-Insight on the score regression task. We compare Q-Insight with handcrafted methods NIQE [28] and BRISQUE [27]; non-MLLM deep-learning methods including NIMA [44],

Table 2: **PLCC / SRCC comparison on the score regression tasks** between our Q-Insight and other competitive IQA methods. All methods except handcrafted ones are trained on the KonIQ dataset. Our Q-Insight outperforms all baseline methods across nearly all benchmarks.

Category	Methods	KonIQ	SPAQ	KADID	PIPAL	LiveW	AGIQA	CSIQ	AVG.
Handcrafted	NIQE [28]	0.533	0.679	0.468	0.195	0.493	0.560	0.718	0.521
	(SPL 2012)	/0.530	/0.664	/0.405	/0.161	/0.449	/0.533	/0.628	/0.481
	BRISQUE [27]	0.225	0.490	0.429	0.267	0.361	0.541	0.740	0.436
	(TIP 2012)	/0.226	/0.406	/0.356	/0.232	/0.313	/0.497	/0.556	/0.369
Non-MLLM Deep-learning	NIMA [44]	0.896	0.838	0.532	0.390	0.814	0.715	0.695	0.697
	(TIP 2018)	/0.859	/0.856	/0.535	/0.399	/0.771	/0.654	/0.649	/0.675
	HyperIQA [41]	0.917	0.791	0.506	0.410	0.772	0.702	0.752	0.693
	(CVPR 2020)	/0.906	/0.788	/0.468	/0.403	/0.749	/0.640	/0.717	/0.667
	DBCNN [65]	0.884	0.812	0.497	0.384	0.773	0.730	0.586	0.667
	(TCSVT 2020)	/0.875	/0.806	/0.484	/0.381	/0.755	/0.641	/0.572	/0.645
	MUSIQ [18]	0.924	0.868	0.575	0.431	0.789	0.722	0.771	0.726
	(ICCV 2021)	/0.929	/0.863	/0.556	/0.431	/0.830	/0.630	/0.710	/0.707
	CLIP-IQA+ [46]	0.909	0.866	0.653	0.427	0.832	0.736	0.772	0.742
	(AAAI 2023)	/0.895	/0.864	/0.654	/0.419	/0.805	/0.685	/0.719	/0.720
ManIQA [54]	0.849	0.768	0.499	0.457	0.849	0.723	0.623	0.681	
(CVPR 2022)	/0.834	/0.758	/0.465	/0.452	/0.832	/0.636	/0.627	/0.658	
MLLM-based	C2Score [73]	0.923	0.867	0.500	0.354	0.786	0.777	0.735	0.706
	(NeurIPS 2024)	/0.910	/0.860	/0.453	/0.342	/0.772	/0.671	/0.705	/0.673
	Qwen-SFT [1]	0.889	0.874	0.668	0.473	0.734	0.813	0.674	0.732
	(Arxiv 2025)	/0.866	/0.875	/0.663	/0.442	/0.728	/0.739	/0.650	/0.709
	Q-Align [51]	0.941	0.886	0.674	0.403	0.853	0.772	0.671	0.705
	(ICML 2024)	/0.940	/0.887	/0.684	/0.419	/0.860	/0.735	/0.737	/0.752
	DeQA [56]	0.953	0.895	0.694	0.472	0.892	0.809	0.787	0.786
	(CVPR 2025)	/0.941	/0.896	/0.687	/0.478	/0.879	/0.729	/0.744	/0.765
	Q-Insight (Ours)	0.933	0.907	0.742	0.486	0.893	0.811	0.870	0.806
	/0.916	/0.905	/0.736	/0.474	/0.865	/0.764	/0.824	/0.783	

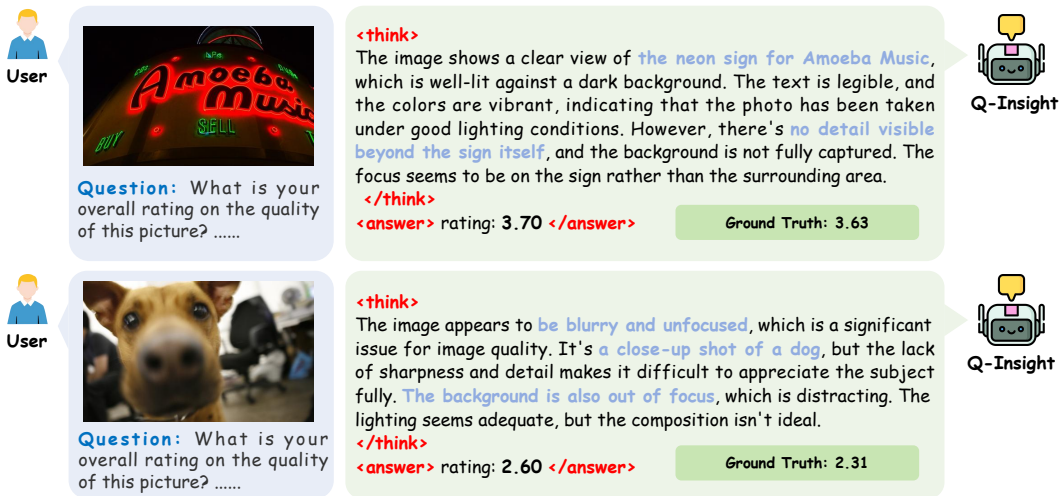


Figure 3: **Score rating and explanation results of our Q-Insight.** Q-Insight is capable of recognizing text, analyzing the lighting and shading conditions of an image, and understanding its composition.

HyperIQA [41], DBCNN [65], MUSIQ [18], CLIP-IQA+ [46], and ManIQA [54]; and recent MLLM-based methods such as C2Score [73], Q-Align [51], DeQA-Score [56], and a supervised fine-tuned Qwen [1]. For a fair comparison, all methods (except handcrafted ones) are trained on the KonIQ dataset, and all MLLM-based methods utilize approximately 7B parameters. The comparison results in terms of PLCC and SRCC between Q-Insight and other IQA methods are presented in Tab. 2. Compared with the state-of-the-art method DeQA-Score, our Q-Insight performs slightly worse on the

Table 3: **Distortion prediction accuracy (Deg. Acc.) and degradation level accuracy (Lev. Acc.)** comparison between our Q-Inspight and AgenticIR [74]. Our method outperforms AgenticIR across all degradations, especially in Noise and JPEG Compression.

Method	Metrics	Noise	Blur	JPEG	Darken	Null	Average
AgenticIR [74] (ICLR 2025)	Deg. Acc.	<u>0.4646</u>	<u>0.8390</u>	<u>0.0135</u>	<u>0.7478</u>	0.9339	<u>0.5998</u>
	Lev. Acc.	<u>0.1858</u>	<u>0.3219</u>	<u>0.0000</u>	<u>0.2611</u>	-	<u>0.1922</u>
Q-Inspight (Ours)	Deg. Acc.	1.0000	0.9756	1.0000	0.9027	<u>0.7603</u>	0.9277
	Lev. Acc.	0.5973	0.4438	0.5541	0.3230	-	0.4796

Table 4: **Ablation study on the score regression task** between multi-task and single-task training. Ours with joint-training significantly outperforms score-only training on PLCC / SRCC metrics.

Method	KonIQ	SPAQ	KADID	PIPAL	LiveW	AGIQA	CSIQ	AVG.
Ours	<u>0.918</u>	<u>0.903</u>	<u>0.702</u>	<u>0.458</u>	<u>0.870</u>	0.816	<u>0.685</u>	<u>0.765</u>
(Score-Only)	<u>/0.895</u>	<u>/0.899</u>	<u>/0.702</u>	<u>/0.435</u>	<u>/0.839</u>	/0.766	<u>/0.640</u>	<u>/0.739</u>
Ours	0.933	0.907	0.742	0.486	0.893	<u>0.811</u>	0.870	0.806
(Joint-Training)	/0.916	/0.905	/0.736	/0.474	/0.865	<u>/0.764</u>	/0.824	/0.783

Table 5: **Ablation study on the degradation perception task** between multi-task and single-task training. Jointly training with score regression improves the accuracy of degradation perception.

Method	Metrics	Noise	Blur	JPEG	Darken	Null	Average
Ours (Degradation-Only)	Deg. Acc.	<u>0.9867</u>	<u>0.9268</u>	<u>0.9685</u>	<u>0.8805</u>	<u>0.5702</u>	<u>0.8960</u>
	Lev. Acc.	<u>0.4343</u>	<u>0.3951</u>	<u>0.3108</u>	<u>0.2567</u>	-	<u>0.3492</u>
Ours (Joint-Training)	Deg. Acc.	1.0000	0.9756	1.0000	0.9027	0.7603	0.9277
	Lev. Acc.	0.5973	0.4438	0.5541	0.3230	-	0.4796

in-domain KonIQ dataset. However, **on out-of-distribution (OOD) datasets, Q-Inspight consistently outperforms all baseline methods across nearly all benchmarks**, achieving approximately 0.2 improvements in both PLCC and SRCC. This demonstrates the effectiveness and strong generalization capability of our approach. Fig. 3 shows two illustrative cases of the reasoning process in the score regression task. Notably, our Q-Inspight does not merely output a numerical score; it also provides a comprehensive and detailed reasoning process. In the first example (top of Fig. 3), Q-Inspight successfully recognizes the text on the neon sign and carefully analyzes details such as lighting conditions. Similarly, the second example (bottom of Fig. 3) highlights Q-Inspight’s capability in understanding image composition. This further demonstrates that Q-Inspight moves beyond merely regressing scores, critically analyzing image quality issues from multiple perspectives, and advancing toward a more comprehensive understanding of image quality.

4.3 Distortion Perception

We further evaluate Q-Inspight on the distortion perception task, comparing it with AgenticIR [74], which fine-tunes an MLLM to perform a similar distortion prediction function. The comparative results are presented in Tab. 3. Notably, AgenticIR requires sequential queries for each possible distortion type, whereas Q-Inspight identifies distortion types **using only a single query**. Q-Inspight consistently outperforms AgenticIR across nearly all distortion categories, resulting in significantly higher average accuracy. However, for the “null” category (no distortion), our performance is slightly lower than AgenticIR, possibly because the reasoning mechanism of Q-Inspight is more sensitive to the presence of potential distortions. Overall, these results highlight Q-Inspight’s ability to efficiently and accurately perceive image distortions through a concise and unified reasoning framework.

4.4 Ablation Studies

Effect of multi-task training. To demonstrate the effectiveness of multi-task training, we compare our jointly trained Q-Inspight with two single-task variants, trained separately on each task. The comparison results are presented in Tabs. 4 and 5. As shown in Tab. 4, the jointly trained Q-Inspight significantly outperforms the score-only variant on nearly all datasets, particularly those with synthetic

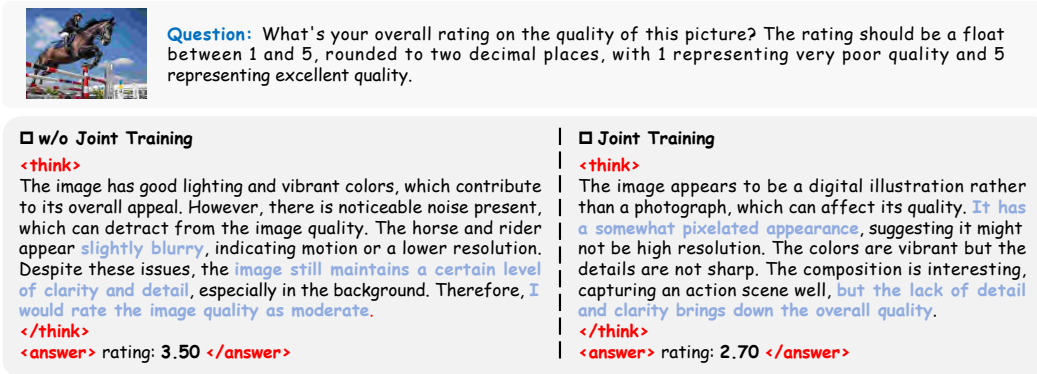


Figure 4: **Subjective ablation comparison** between joint multi-task training and w/o joint training on the explanation of image scoring. With joint training, our method can better perceive degradation cues in images (such as pixelated appearance), thereby improving the accuracy of quality assessment.

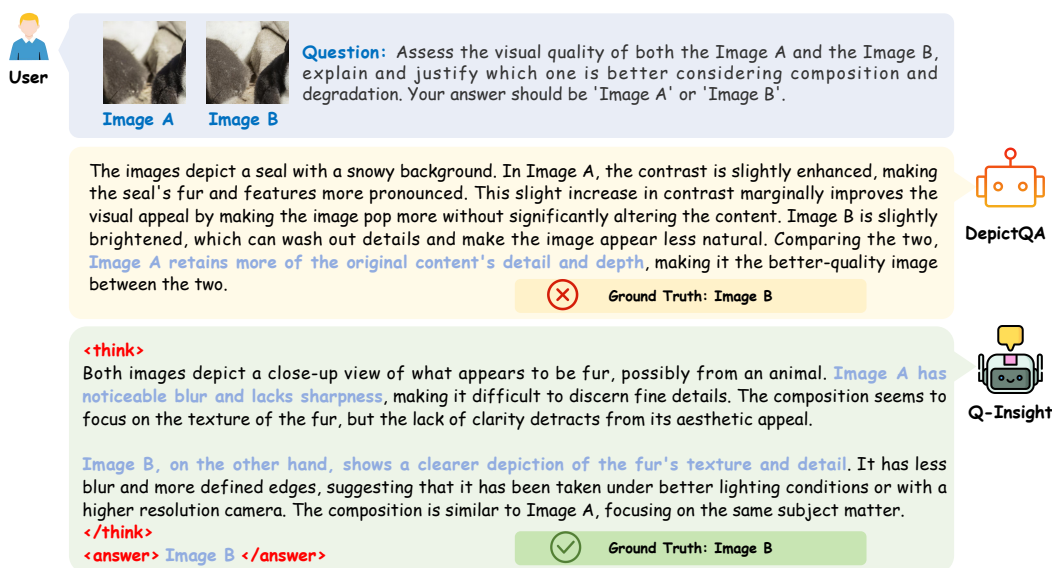


Figure 5: **Image comparison reasoning results** of our Q-Inspight and DepictQA [58, 57]. Q-Inspight outperforms DepictQA in comprehensive content understanding and accurate degradation perception.

distortions (KADID, CSIQ) and model-processed distortions (PIPAL). This clearly indicates that incorporating the degradation perception task benefits the score regression task. Fig. 4 further illustrates the importance of multi-task training: Q-Inspight can better perceive detailed degradations such as pixel-level artifacts, thus enhancing overall accuracy in quality assessment. Similarly, Tab. 5 demonstrates that in the degradation perception task, the jointly trained model outperforms the degradation-only variant across all distortion categories. This suggests that the score regression task also positively contributes to the degradation perception capability. These results confirm the mutual benefit and effectiveness of our multi-task training approach. Furthermore, this clearly demonstrates that the visual quality understanding potential of MLLMs can be significantly enhanced through carefully designed training tasks and objectives.

4.5 Zero-Shot Image Comparison Reasoning

Our Q-Inspight effectively generalizes to zero-shot image comparison reasoning tasks, covering both reference-based and non-reference-based scenarios, as illustrated in Figs. 1 and 5. In Fig. 1, Q-Inspight conducts a reference-based comparison, where the reference image is of lower quality, and Images A and B are outputs from different super-resolution methods. Q-Inspight compares these two images from both fidelity and overall quality perspectives, demonstrating its potential utility in image enhancement tasks. In Fig. 5, Q-Inspight surpasses DepictQA [58, 57] in terms of

comprehensive content understanding and accurate degradation perception. Importantly, Q-Insight achieves this without relying on specialized training on large-scale textual datasets, highlighting its strong generalization ability enabled by the GRPO-based framework and multi-task training strategy.

5 Conclusion

In this paper, we introduce Q-Insight, a novel GRPO-based model for comprehensive image quality understanding. It jointly optimizes score regression and degradation perception tasks using only a limited amount of labeled data. Unlike traditional methods that rely on extensive textual annotations or purely numerical scoring, our framework combines numerical accuracy with interpretative reasoning, significantly improving the perceptual analysis capabilities of image quality models. Extensive experiments show that Q-Insight consistently outperforms existing state-of-the-art methods across various datasets and tasks, demonstrating impressive zero-shot generalization to image comparison reasoning. Looking ahead, Q-Insight can extend its capabilities to a wide range of tasks, such as image aesthetic assessments, and serve as a powerful discriminative signal to improve image enhancement models. As a unified model for scoring, perception, comparison, and reasoning, Q-Insight can act as a central hub, coordinating image reconstruction tools and providing valuable insights into the enhancement process. This integrated and automated system has the potential to revolutionize image quality understanding and enhancement, providing a unified solution that can transform how image quality is evaluated, improved, and applied across various fields.

References

- [1] Shuai Bai, Keqin Chen, Xuejing Liu, Jialin Wang, Wenbin Ge, Sib0 Song, Kai Dang, Peng Wang, Shijie Wang, Jun Tang, et al. Qwen2. 5-vl technical report. *arXiv preprint arXiv:2502.13923*, 2025.
- [2] Yuntao Bai, Saurav Kadavath, Sandipan Kundu, Amanda Askell, Jackson Kernion, Andy Jones, Anna Chen, Anna Goldie, Azalia Mirhoseini, Cameron McKinnon, et al. Constitutional ai: Harmlessness from ai feedback. *arXiv preprint arXiv:2212.08073*, 2022.
- [3] Sebastian Bosse, Dominique Maniry, Klaus-Robert Müller, Thomas Wiegand, and Wojciech Samek. Deep neural networks for no-reference and full-reference image quality assessment. *IEEE Transactions on image processing*, 27(1):206–219, 2017.
- [4] Yue Cao, Zhaolin Wan, Dongwei Ren, Zifei Yan, and Wangmeng Zuo. Incorporating semi-supervised and positive-unlabeled learning for boosting full reference image quality assessment. In *Proceedings of the IEEE/CVF conference on computer vision and pattern recognition*, pages 5851–5861, 2022.
- [5] Chaofeng Chen, Sensen Yang, Haoning Wu, Liang Liao, Zicheng Zhang, Annan Wang, Wenxiu Sun, Qiong Yan, and Weisi Lin. Q-ground: Image quality grounding with large multi-modality models. In *Proceedings of the 32nd ACM International Conference on Multimedia*, pages 486–495, 2024.
- [6] Paul F Christiano, Jan Leike, Tom Brown, Miljan Martic, Shane Legg, and Dario Amodei. Deep reinforcement learning from human preferences. *Advances in neural information processing systems*, 30, 2017.
- [7] Prafulla Dhariwal and Alexander Nichol. Diffusion models beat gans on image synthesis. *Advances in neural information processing systems*, 34:8780–8794, 2021.
- [8] Keyan Ding, Yi Liu, Xueyi Zou, Shiqi Wang, and Kede Ma. Locally adaptive structure and texture similarity for image quality assessment. In *Proceedings of the 29th ACM International Conference on multimedia*, pages 2483–2491, 2021.
- [9] Keyan Ding, Kede Ma, Shiqi Wang, and Eero P Simoncelli. Image quality assessment: Unifying structure and texture similarity. *IEEE transactions on pattern analysis and machine intelligence*, 44(5):2567–2581, 2020.
- [10] Yuming Fang, Hanwei Zhu, Yan Zeng, Kede Ma, and Zhou Wang. Perceptual quality assessment of smartphone photography. In *Proceedings of the IEEE/CVF conference on computer vision and pattern recognition*, pages 3677–3686, 2020.

- [11] Deepti Ghadiyaram and Alan C Bovik. Live in the wild image quality challenge database. *Online: <http://live.ece.utexas.edu/research/ChallengeDB/index.html> [Mar, 2017]*, 2015.
- [12] Abhijay Ghildyal and Feng Liu. Shift-tolerant perceptual similarity metric. In *European Conference on Computer Vision*, pages 91–107. Springer, 2022.
- [13] Haoming GU, Jinjinand Cai, Haoyu Chen, Xiaoxing Ye, Ren Jimmy S, and Chao Dong. Pipal: a large-scale image quality assessment dataset for perceptual image restoration. In *European Conference on Computer Vision*, pages 633–651. Springer, 2020.
- [14] Daya Guo, Dejian Yang, Haowei Zhang, Junxiao Song, Ruoyu Zhang, Runxin Xu, Qihao Zhu, Shirong Ma, Peiyi Wang, Xiao Bi, et al. Deepseek-r1: Incentivizing reasoning capability in llms via reinforcement learning. *arXiv preprint arXiv:2501.12948*, 2025.
- [15] Vlad Hosu, Hanhe Lin, Tamas Sziranyi, and Dietmar Saupe. Koniq-10k: An ecologically valid database for deep learning of blind image quality assessment. *IEEE Transactions on Image Processing*, 29:4041–4056, 2020.
- [16] Binyuan Hui, Jian Yang, Zeyu Cui, Jiayi Yang, Dayiheng Liu, Lei Zhang, Tianyu Liu, Jiajun Zhang, Bowen Yu, Keming Lu, et al. Qwen2. 5-coder technical report. *arXiv preprint arXiv:2409.12186*, 2024.
- [17] Le Kang, Peng Ye, Yi Li, and David Doermann. Convolutional neural networks for no-reference image quality assessment. In *Proceedings of the IEEE conference on computer vision and pattern recognition*, pages 1733–1740, 2014.
- [18] Junjie Ke, Qifei Wang, Yilin Wang, Peyman Milanfar, and Feng Yang. Musiq: Multi-scale image quality transformer. In *Proceedings of the IEEE/CVF international conference on computer vision*, pages 5148–5157, 2021.
- [19] Eric C Larson and Damon M Chandler. Most apparent distortion: full-reference image quality assessment and the role of strategy. *Journal of electronic imaging*, 19(1):011006–011006, 2010.
- [20] Chunyi Li, Zicheng Zhang, Haoning Wu, Wei Sun, Xiongkuo Min, Xiaohong Liu, Guangtao Zhai, and Weisi Lin. Agiqa-3k: An open database for ai-generated image quality assessment. *IEEE Transactions on Circuits and Systems for Video Technology*, 34(8):6833–6846, 2023.
- [21] Hanhe Lin, Vlad Hosu, and Dietmar Saupe. Kadid-10k: A large-scale artificially distorted iqa database. In *2019 Eleventh International Conference on Quality of Multimedia Experience (QoMEX)*, pages 1–3. IEEE, 2019.
- [22] Haotian Liu, Chunyuan Li, Qingyang Wu, and Yong Jae Lee. Visual instruction tuning. *Advances in neural information processing systems*, 36:34892–34916, 2023.
- [23] Xialei Liu, Joost Van De Weijer, and Andrew D Bagdanov. Rankiqa: Learning from rankings for no-reference image quality assessment. In *Proceedings of the IEEE international conference on computer vision*, pages 1040–1049, 2017.
- [24] Ziyu Liu, Zeyi Sun, Yuhang Zang, Xiaoyi Dong, Yuhang Cao, Haodong Duan, Dahua Lin, and Jiaqi Wang. Visual-rft: Visual reinforcement fine-tuning. *arXiv preprint arXiv:2503.01785*, 2025.
- [25] Ilya Loshchilov and Frank Hutter. Decoupled weight decay regularization. *arXiv preprint arXiv:1711.05101*, 2017.
- [26] Chao Ma, Chih-Yuan Yang, Xiaokang Yang, and Ming-Hsuan Yang. Learning a no-reference quality metric for single-image super-resolution. *Computer Vision and Image Understanding*, 158:1–16, 2017.
- [27] Anish Mittal, Anush Krishna Moorthy, and Alan Conrad Bovik. No-reference image quality assessment in the spatial domain. *IEEE Transactions on image processing*, 21(12):4695–4708, 2012.
- [28] Anish Mittal, Rajiv Soundararajan, and Alan C Bovik. Making a “completely blind” image quality analyzer. *IEEE Signal processing letters*, 20(3):209–212, 2012.
- [29] Anush Krishna Moorthy and Alan Conrad Bovik. A two-step framework for constructing blind image quality indices. *IEEE Signal processing letters*, 17(5):513–516, 2010.
- [30] Anush Krishna Moorthy and Alan Conrad Bovik. Blind image quality assessment: From natural scene statistics to perceptual quality. *IEEE transactions on Image Processing*, 20(12):3350–3364, 2011.

- [31] Long Ouyang, Jeffrey Wu, Xu Jiang, Diogo Almeida, Carroll Wainwright, Pamela Mishkin, Chong Zhang, Sandhini Agarwal, Katarina Slama, Alex Ray, et al. Training language models to follow instructions with human feedback. *Advances in neural information processing systems*, 35:27730–27744, 2022.
- [32] Da Pan, Ping Shi, Ming Hou, Zefeng Ying, Sizhe Fu, and Yuan Zhang. Blind predicting similar quality map for image quality assessment. In *Proceedings of the IEEE conference on computer vision and pattern recognition*, pages 6373–6382, 2018.
- [33] Jiazhen Pan, Che Liu, Junde Wu, Fenglin Liu, Jiayuan Zhu, Hongwei Bran Li, Chen Chen, Cheng Ouyang, and Daniel Rueckert. Medvlm-r1: Incentivizing medical reasoning capability of vision-language models (vlms) via reinforcement learning. *arXiv preprint arXiv:2502.19634*, 2025.
- [34] Ekta Prashnani, Hong Cai, Yasamin Mostofi, and Pradeep Sen. Pieapp: Perceptual image-error assessment through pairwise preference. In *Proceedings of the IEEE Conference on Computer Vision and Pattern Recognition*, pages 1808–1817, 2018.
- [35] Robin Rombach, Andreas Blattmann, Dominik Lorenz, Patrick Esser, and Björn Ommer. High-resolution image synthesis with latent diffusion models. In *Proceedings of the IEEE/CVF conference on computer vision and pattern recognition*, pages 10684–10695, 2022.
- [36] Michele A Saad, Alan C Bovik, and Christophe Charrier. Blind image quality assessment: A natural scene statistics approach in the dct domain. *IEEE transactions on Image Processing*, 21(8):3339–3352, 2012.
- [37] Zhihong Shao, Peiyi Wang, Qihao Zhu, Runxin Xu, Junxiao Song, Xiao Bi, Haowei Zhang, Mingchuan Zhang, YK Li, Y Wu, et al. Deepseekmath: Pushing the limits of mathematical reasoning in open language models. *arXiv preprint arXiv:2402.03300*, 2024.
- [38] H Sheikh. Live image quality assessment database release 2. <http://live.ece.utexas.edu/research/quality>, 2005.
- [39] Hamid R Sheikh and Alan C Bovik. Image information and visual quality. *IEEE Transactions on image processing*, 15(2):430–444, 2006.
- [40] David Silver, Julian Schrittwieser, Karen Simonyan, Ioannis Antonoglou, Aja Huang, Arthur Guez, Thomas Hubert, Lucas Baker, Matthew Lai, Adrian Bolton, et al. Mastering the game of go without human knowledge. *nature*, 550(7676):354–359, 2017.
- [41] Shaolin Su, Qingsen Yan, Yu Zhu, Cheng Zhang, Xin Ge, Jinqiu Sun, and Yanning Zhang. Blindly assess image quality in the wild guided by a self-adaptive hyper network. In *Proceedings of the IEEE/CVF conference on computer vision and pattern recognition*, pages 3667–3676, 2020.
- [42] Simeng Sun, Tao Yu, Jiahua Xu, Wei Zhou, and Zhibo Chen. Graphiqa: Learning distortion graph representations for blind image quality assessment. *IEEE Transactions on Multimedia*, 25:2912–2925, 2022.
- [43] Zhiqing Sun, Sheng Shen, Shengcao Cao, Haotian Liu, Chunyuan Li, Yikang Shen, Chuang Gan, Liang-Yan Gui, Yu-Xiong Wang, Yiming Yang, et al. Aligning large multimodal models with factually augmented rlhf. *arXiv preprint arXiv:2309.14525*, 2023.
- [44] Hossein Talebi and Peyman Milanfar. Nima: Neural image assessment. *IEEE transactions on image processing*, 27(8):3998–4011, 2018.
- [45] Hugo Touvron, Thibaut Lavril, Gautier Izacard, Xavier Martinet, Marie-Anne Lachaux, Timothée Lacroix, Baptiste Rozière, Naman Goyal, Eric Hambro, Faisal Azhar, et al. Llama: Open and efficient foundation language models. *arXiv preprint arXiv:2302.13971*, 2023.
- [46] Jianyi Wang, Kelvin CK Chan, and Chen Change Loy. Exploring clip for assessing the look and feel of images. In *Proceedings of the AAAI conference on artificial intelligence*, volume 37, pages 2555–2563, 2023.
- [47] Zhou Wang, Alan C Bovik, Hamid R Sheikh, and Eero P Simoncelli. Image quality assessment: from error visibility to structural similarity. *IEEE transactions on image processing*, 13(4):600–612, 2004.
- [48] Haoning Wu, Zicheng Zhang, Erli Zhang, Chaofeng Chen, Liang Liao, Annan Wang, Chunyi Li, Wenxiu Sun, Qiong Yan, Guangtao Zhai, et al. Q-bench: A benchmark for general-purpose foundation models on low-level vision. *arXiv preprint arXiv:2309.14181*, 2023.

- [49] Haoning Wu, Zicheng Zhang, Erli Zhang, Chaofeng Chen, Liang Liao, Annan Wang, Kaixin Xu, Chunyi Li, Jingwen Hou, Guangtao Zhai, et al. Q-instruct: Improving low-level visual abilities for multi-modality foundation models. In *Proceedings of the IEEE/CVF conference on computer vision and pattern recognition*, pages 25490–25500, 2024.
- [50] Haoning Wu, Zicheng Zhang, Erli Zhang, Chaofeng Chen, Liang Liao, Annan Wang, Kaixin Xu, Chunyi Li, Jingwen Hou, Guangtao Zhai, et al. Q-instruct: Improving low-level visual abilities for multi-modality foundation models. In *Proceedings of the IEEE/CVF conference on computer vision and pattern recognition*, pages 25490–25500, 2024.
- [51] Haoning Wu, Zicheng Zhang, Weixia Zhang, Chaofeng Chen, Liang Liao, Chunyi Li, Yixuan Gao, Annan Wang, Erli Zhang, Wenxiu Sun, et al. Q-align: Teaching llms for visual scoring via discrete text-defined levels. *arXiv preprint arXiv:2312.17090*, 2023.
- [52] Haoning Wu, Hanwei Zhu, Zicheng Zhang, Erli Zhang, Chaofeng Chen, Liang Liao, Chunyi Li, Annan Wang, Wenxiu Sun, Qiong Yan, et al. Towards open-ended visual quality comparison. In *European Conference on Computer Vision*, pages 360–377. Springer, 2024.
- [53] An Yang, Beichen Zhang, Binyuan Hui, Bofei Gao, Bowen Yu, Chengpeng Li, Dayiheng Liu, Jianhong Tu, Jingren Zhou, Junyang Lin, et al. Qwen2. 5-math technical report: Toward mathematical expert model via self-improvement. *arXiv preprint arXiv:2409.12122*, 2024.
- [54] Sidi Yang, Tianhe Wu, Shuwei Shi, Shanshan Lao, Yuan Gong, Mingdeng Cao, Jiahao Wang, and Yujiu Yang. Maniqa: Multi-dimension attention network for no-reference image quality assessment. In *Proceedings of the IEEE/CVF conference on computer vision and pattern recognition*, pages 1191–1200, 2022.
- [55] Huaiyuan Ying, Shuo Zhang, Linyang Li, Zhejian Zhou, Yunfan Shao, Zhaoye Fei, Yichuan Ma, Jiawei Hong, Kuikun Liu, Ziyi Wang, et al. Internlm-math: Open math large language models toward verifiable reasoning. *arXiv preprint arXiv:2402.06332*, 2024.
- [56] Zhiyuan You, Xin Cai, Jinjin Gu, Tianfan Xue, and Chao Dong. Teaching large language models to regress accurate image quality scores using score distribution. *arXiv preprint arXiv:2501.11561*, 2025.
- [57] Zhiyuan You, Jinjin Gu, Zheyuan Li, Xin Cai, Kaiwen Zhu, Chao Dong, and Tianfan Xue. Descriptive image quality assessment in the wild. *arXiv preprint arXiv:2405.18842*, 2024.
- [58] Zhiyuan You, Zheyuan Li, Jinjin Gu, Zhenfei Yin, Tianfan Xue, and Chao Dong. Depicting beyond scores: Advancing image quality assessment through multi-modal language models. In *European Conference on Computer Vision*, pages 259–276. Springer, 2024.
- [59] Tianyu Yu, Yuan Yao, Haoye Zhang, Taiwen He, Yifeng Han, Ganqu Cui, Jinyi Hu, Zhiyuan Liu, Hai-Tao Zheng, Maosong Sun, et al. Rllm-v: Towards trustworthy llms via behavior alignment from fine-grained correctional human feedback. In *Proceedings of the IEEE/CVF Conference on Computer Vision and Pattern Recognition*, pages 13807–13816, 2024.
- [60] Tianyu Yu, Haoye Zhang, Yuan Yao, Yunkai Dang, Da Chen, Xiaoman Lu, Ganqu Cui, Taiwen He, Zhiyuan Liu, Tat-Seng Chua, et al. Rllm-v: Aligning llms through open-source ai feedback for super gpt-4v trustworthiness. *arXiv preprint arXiv:2405.17220*, 2024.
- [61] Jingyi Zhang, Jiaxing Huang, Huanjin Yao, Shunyu Liu, Xikun Zhang, Shijian Lu, and Dacheng Tao. R1-vl: Learning to reason with multimodal large language models via step-wise group relative policy optimization. *arXiv preprint arXiv:2503.12937*, 2025.
- [62] Lin Zhang, Lei Zhang, and Alan C Bovik. A feature-enriched completely blind image quality evaluator. *IEEE Transactions on Image Processing*, 24(8):2579–2591, 2015.
- [63] Lin Zhang, Lei Zhang, Xuanqin Mou, and David Zhang. Fsim: A feature similarity index for image quality assessment. *IEEE transactions on Image Processing*, 20(8):2378–2386, 2011.
- [64] Richard Zhang, Phillip Isola, Alexei A Efros, Eli Shechtman, and Oliver Wang. The unreasonable effectiveness of deep features as a perceptual metric. In *Proceedings of the IEEE conference on computer vision and pattern recognition*, pages 586–595, 2018.
- [65] Weixia Zhang, Kede Ma, Jia Yan, Dexiang Deng, and Zhou Wang. Blind image quality assessment using a deep bilinear convolutional neural network. *IEEE Transactions on Circuits and Systems for Video Technology*, 2020.
- [66] Yuxiang Zhang, Shangxi Wu, Yuqi Yang, Jiangming Shu, Jinlin Xiao, Chao Kong, and Jitao Sang. o1-coder: an o1 replication for coding. *arXiv preprint arXiv:2412.00154*, 2024.

- [67] Zicheng Zhang, Ziheng Jia, Haoning Wu, Chunyi Li, Zijian Chen, Yingjie Zhou, Wei Sun, Xiaohong Liu, Xionghuo Min, Weisi Lin, et al. Q-bench-video: Benchmarking the video quality understanding of llms. *arXiv preprint arXiv:2409.20063*, 2024.
- [68] Zicheng Zhang, Tengchuan Kou, Shushi Wang, Chunyi Li, Wei Sun, Wei Wang, Xiaoyu Li, Zongyu Wang, Xuezhi Cao, Xionghuo Min, et al. Q-eval-100k: Evaluating visual quality and alignment level for text-to-vision content. *arXiv preprint arXiv:2503.02357*, 2025.
- [69] Zicheng Zhang, Haoning Wu, Ziheng Jia, Weisi Lin, and Guangtao Zhai. Teaching llms for image quality scoring and interpreting. *arXiv preprint arXiv:2503.09197*, 2025.
- [70] Zhiyuan Zhao, Bin Wang, Linke Ouyang, Xiaoyi Dong, Jiaqi Wang, and Conghui He. Beyond hallucinations: Enhancing llms through hallucination-aware direct preference optimization. *arXiv preprint arXiv:2311.16839*, 2023.
- [71] Heliang Zheng, Huan Yang, Jianlong Fu, Zheng-Jun Zha, and Jiebo Luo. Learning conditional knowledge distillation for degraded-reference image quality assessment. In *Proceedings of the IEEE/CVF International Conference on Computer Vision*, pages 10242–10251, 2021.
- [72] Hancheng Zhu, Leida Li, Jinjian Wu, Weisheng Dong, and Guangming Shi. Metaiq: Deep meta-learning for no-reference image quality assessment. In *Proceedings of the IEEE/CVF conference on computer vision and pattern recognition*, pages 14143–14152, 2020.
- [73] Hanwei Zhu, Haoning Wu, Yixuan Li, Zicheng Zhang, Baoliang Chen, Lingyu Zhu, Yuming Fang, Guangtao Zhai, Weisi Lin, and Shiqi Wang. Adaptive image quality assessment via teaching large multimodal model to compare. In *The Thirty-eighth Annual Conference on Neural Information Processing Systems*, 2024.
- [74] Kaiwen Zhu, Jinjin Gu, Zhiyuan You, Yu Qiao, and Chao Dong. An intelligent agentic system for complex image restoration problems. *arXiv preprint arXiv:2410.17809*, 2024.